International Journal of Scientific Research and Engineering Development-– Volume 3 Issue 4, July –Aug 2020

Available at www.ijsred.com

RESEARCH ARTICLE OPEN ACCESS

Extinction of Millimeter wave on Two Dimensional Slices of Foam-Covered Sea-surface

Ayibapreye Kelvin BENJAMIN*, Collins E. OUSERIGHA**

*Department of Electrical/Electronic Engineering, Niger Delta University, P.M.B 071 Yenagoa, Bayelsa State Nigeria

Email:ayibapreyebenjamin@ndu.edu.ng

** Department of Physics, Niger Delta University, P.M.B 071 Yenagoa, Bayelsa State, Nigeria

Email:ouserigha.ec@ndu.edu.ng

----------**********----------

Abstract:

This paper focuses on investigation of millimeter wave (mmW) extinction due to its interaction with 2-D layers of randomly distributed air-bubbles on the surface of the ocean. The Split-step Fourier method was adopted for evaluation of the refractive and diffractive effects of scattered mmW due to its interaction with layers of foam-covered sea-surface. With known varying effective dielectric constant of closely packed air-bubbles in these layers, estimates of millimetre wave attenuation through layers of sea-foams as functions of frequency, foam layer thickness, polarization and angle of incidence are reported.

Keywords **—Extinction, Sea-foams, Split-step Fourier method.**

----------**********----------

I. INTRODUCTION

Due to the incessant demand for precision and accurate prediction of climate and weather variables from passive radiometric measurements at WindSat frequencies, there is need investigate the direct and indirect effects of air-bubbles (sea-foams) interactions with millimeter wave at the air-seawater interface. Evaluation of extinction of millimeter wave by a flat sea-surface covered by foam is a significant research problem which contributes vastly in satellite-based geophysical retrievals of environmental variables such as sea surface temperature, sea surface emissivity and brightness temperature.

Anguelova et.al asserted that bubble plumes in seawater forms foam layers at the sea surface and in some instances sea spray suspended closely above sea surface. The skin depth of sea foam at microwave frequency narrows the remote sensing investigations of the sea foam to its surface expression [1]. Many air-sea interaction processes are quantified in terms of whitecap fraction W because oceanic whitecaps are the most visible and direct way of observing breaking of wind waves in the open ocean. Enhanced by breaking waves, surface fluxes of momentum, heat, and mass are critical for ocean atmosphere coupling and thus affect the accuracy of models used to forecast weather and predict storm intensification and climate change. Whitecap fraction is defined as the fraction of a unit sea surface covered by foam [2]. It has been traditionally measured by extracting the high intensity pixels marking white water in still photographs or video images collected from towers, ships, and aircrafts. Satellite-based passive remote sensing of whitecap fraction is a recent development that allows long term, consistent observations of white capping on a global scale. The remote sensing method relies on change of ocean surface emissivity at microwave frequencies

(e.g., 6 to 37GHz) due to the presence of sea foam on a rough sea surface. These changes at the ocean surface are observed from the satellite as brightness temperatureT_B [3]-[4].

The algorithm to obtain W from satellite observations of T_B was developed at the Naval Research Laboratory within the framework of WindSat mission. It improved upon the feasibility study of this remote sensing technique by using independent sources for the input variables of the algorithm, physically based models for the emissivity of rough sea surface and emissivity of foam, improved rain flag, and improved atmospheric model necessary for the atmospheric correction. The database built with this algorithm compiles W for entire year 2006 matched in time and space with data for the wind vector, wave field (such as significant wave height and peak wave period), and environmental parameters (such as sea surface temperature and atmospheric stability). This data base has proved useful in analysing and quantifying the variability of W. Magdalena et.al presented an updated algorithm for estimating W from WindSat T_B data using new sources and products for the input variables. This approach replaces the originally used QuikSCAT data for ocean wind vector are replaced with new wind vector fields [3]-[4].

Xiaobin Tin et.al found large discrepancies when comparing measurements and model simulations as wind speed (WS) rise above $12ms^{-1}$. Over the open ocean and for moderately wind speeds (WS_s), the Soil Moisture and Ocean Salinity (SMOS) brightness temperature (T_B) was initially consistent with T_B computations made by theoretical prelaunch models implemented in European Space Level 2 Ocean Salinity processor [5]. In [5] a new approach was proposed using new set of parameters for sea wave spectrum and foam coverage model that can be used for simulating L-band radiometer data over a large range of WS based on the deduction of wind induced components from the SMOS data.

[6]-[7] used Monte Carlo Simulation and the dense radiative transfer theory (DMRT) with quasi-crystalline approximation (QCA) to evaluate direct and inverse scattering problems. The Monte Carlo simulation use an exact numerical formulation based on Foldy-Lax multiple scattering equations of 3-D Maxwell's equation. Previous calculations assumed particles with size parameter ($ka \ll 1$) using DMRT. An extension to moderate sized particle is vital for millimetre wave remote sensing because high frequency range above 10GHz, the particle size in geographical media are comparable to the wavelength (Mie Scattering). Contributions by Chi-Te Chan et.al shows that analytical results were consistent with Monte Carlo simulations of exact solutions of Maxwell's equations of randomly distributed finite size sphere without adjusting parameters. Input parameters of the model are all physical parameters of sizes, concentrations (volume fractions) and permittivity. The results of the models were used to obtain brightness temperatures in passive remote sensing of ocean foam at 19GHz and 37GHz.

Mie scattering could be used with QCA and QCA-CP (quasi-crystalline approximation with coherent potential) to provide solution that is consistent for particle sizes comparable to or larger than the wavelength. With results obtained from [7], the extinction behaviour of sea foam was illustrated, thermal emission from sea foam was evaluated and it was shown that the extinction was dominated by absorption. A physical model of foam emission was obtained that relates observed brightness temperature to the microstructure of foam as well as ocean surface wind vector. The brightness temperature of sea form can be presented as a function of observed angle and frequency and radiative transfer equation could be solved using derived QCA parameters.

II. ESTIMATE OF THE EFFECTIVE DIELECTRIC CONSTANT OF SEA-FORMS

Figures A-E of [8] comprise of 3D (three dimensions) slices of randomly packed spheres in a

unit cube. These slices were later translated to 2D slices of randomly packed circles. The conversion of 3D randomly packed spheres to 2D packed circle was achieved by calculating the radii of each individual circle using the concept of intersection of a sphere and a plane. The 2D slices were discretized with grid sizes Δx and Δy which leads to intersection of the circles bounded in a unit square with some grid points. The grid sizes were sampled such that the edges of the circles circumference which intersects with grid points farther from the inner grids bounded by the circles are negligible.

Estimate of the effective dielectric constant of sea foams were made by modelling the randomly packed bubbles as concentric circles in 2-D where the outer circle is a mixture of air and seawater while the inner circle contains about $(80-95)$ % air, with these estimates we were able to calculate the area of the annulus (ring) as the radii of the outer circles are known.

Table 1 and 2 of [8] illustrate dielectric constant of seawater at fixed salinity $34\ psu$ and sea surface temperature $20°C$. The dielectric constant of air is taken as $1.00005 + 0.0000i$. The area of the circles in each slice was calculated using the total number of grid points. The sea-foam effective dielectric constants at WindSat frequencies $6.8\ GHz$, $18.7\ GHz$, and $23.8\ GHz$ were calculated for five slices of randomly packed spherical air-bubbles that are coated with thin layers of seawater.

TABLE I
Results for Dielectric constant of sea foam at frequencies of $6.8\ GHz$, $18.7\ GHz$ and $23.8\ GHz$ for 5 2-D Slices of randomly packed air-bubbles covered with thin-layer of seawater.

FREQUENCY	$6.8\ GHz$	$18.7\ GHz$	$23.8\ GHz$
Slice 1	$1.1294 + 0.1297i$	$1.0657 + 0.0896i$	$1.0008 + 0.1267i$
Slice 2	$1.2032 + 0.1562i$	$1.0937 + 0.1460i$	$1.0117 + 0.1526i$
Slice 3	$1.2122 + 0.1537i$	$1.1252 + 0.1652i$	$1.0263 + 0.1833i$
Slice 4	$1.3060 + 0.2148i$	$1.2094 + 0.1804i$	$1.0427 + 0.2098$
Slice 5	$1.3457 + 0.2357i$	$1.2547 + 0.1993i$	$1.0567 + 0.2302i$

III. PARABOLIC WAVE EQUATION METHOD

Parabolic wave equation method is one of the numerous computational and numerical approximations used in modelling the interaction of EM fields with physical objects and the environment. Parabolic equation method (PEM) provides efficient approximation to the Helmholtz wave equation which is derived by decoupling of Maxwell's equations to evaluate radio-wave propagation in random and inhomogeneous media.

Leontovich and Fock [9,10] introduced the parabolic wave equation which is very powerful in its application for analysing the problem of radio-wave diffraction around the earth or in the atmosphere. [11] Malyuzhinets, Fock and Wainstein generalized the PEM based on studies of ray-coordinates and transverse diffusion. Malyuzhinets unified geometric optics with the parabolic approximate method to establish an efficient theory of diffraction of obstacles. Tappert et.al [9-11] developed the very powerful split-step Fourier solution of the parabolic equation for solving underwater acoustic problems.

PEM applications spans from radio-waves propagation problems in VHF to millimetre wave affected by atmospheric refraction, diffraction and reflection by irregular terrains and rough sea surface. More reviews and references of the parabolic equation method can be accessed in [11] and [9-12].

The principal advantages of the various parabolic wave equations derived below is that it constitutes an initial value problem in range and hence can be solved by a range matching numerical technique, given a source field distribution over depth at the initial range.

Over the years, several different solution techniques have been implemented in computer codes [9-12], but only the split-step Fourier technique and various finite-difference / finite-element techniques have gained widespread use in the underwater acoustic community.

Before going into details on the numerical solution schemes, let us briefly point out some advantages

and disadvantages of these two main solution techniques.

The split-step algorithm has been extensively used to solve the SPE ever since it was developed by Hardin and Tappert [9] in the early 1970s. The technique is computationally efficient for long-range, narrow-angle propagation problems with negligible bottom interactions.

For short-range, deep water problems and shallow water problems in general, propagation is basically more wide-angled and bottom interacting paths become more important.

This requires the use of wide-angle PEs, which can be solved only by finite difference or finite elements. Moreover, the strong speed and density contrasts encountered at the water-bottom interface adversely affect the computational efficiency of the split-step technique, which in cases of strong bottom interaction requires an excessively fine computational grid$(\Delta x, z)$. Hence, the advantage of higher computational efficiency of the split-step technique is entirely lost in situations with strong bottom interactions.

Finite-difference and Finite-element solutions are applicable to PE for arbitrary large angles. The main drawback of these schemes is that, for long range the split-step solution is more efficient and also for narrow angle with minimal or no bottom interaction. The split-step solution remains the most adopted technique for performance prediction as it is more suitable to solving many practical ocean surface problems.

Conversely, the finite-difference and finite-element schemes have widespread application for wide-angle and bottom interacting boundaries. It is prominent for providing higher accuracy in these domains.

The most recent development in terms of efficient PE solution schemes is a split-step Pade' approximations derived by Collins [13,14]. He uses higher order Pade' approximations not the square root operators. The result is a considerable efficiency gain through the use of higher range step. Thus, the scheme is claimed to be more than an order of magnitude faster than standard FD/FE solution techniques. This could create a unified PE solution approach where the accurate high angle PEs can be solved with the efficiency of the classical split-step Fourier scheme.

IV. DERIVATION OF THE PARABOLIC WAVE EQUATION

Using a simple model which describe the propagation of a reduced function

$$\psi(x,z) = u(x,z)e^{ikx} \quad (1)$$

associated with the direction of propagation x.

Where $u(x,z)$ can be expressed as

$$u(x,z) = \Psi(x,z)e^{-ikx} \quad (2)$$

The Helmholtz equation of the reduced function is obtained by decoupling Maxwell's equations and can be expressed as

$$\nabla^2\Psi + k^2n^2(x,z)\Psi = 0 \quad (3)$$

Where $n^2(x,z)$ is the refractive index and k is the wavenumber. The refractive index $n^2(x,z)$ is assumed to possess smooth variations. The reduced function implies that the propagation energy varies slowly at angles close to the paraxial direction.

The Laplacian of $\Psi(x,z)$ can be expressed as

$$\nabla^2\Psi = [\nabla^2u + 2ik\nabla u - k^2u]e^{ikx} \quad (4)$$

Where Ψ is taken as the product of a plane wave solution, substituting equation (4) into equation (3) yields

$$[\nabla^2u + 2ik\nabla u - k^2u]e^{ikx} + k^2n^2(x,z)\,ue^{ikx} = 0 \quad (5)$$

$$\nabla^2u + 2ik\nabla u + k^2n^2\{(x,z) - 1\}\,u = 0 \quad (6)$$

The Laplacian operator for 2D can be expressed as $(\frac{\partial^2}{\partial x^2} + \frac{\partial^2}{\partial z^2})$, in the atmosphere where $n-1$ is small, we neglect $\frac{\partial^2}{\partial x^2}$ as small (paraxial approximation) and equation (6) becomes

$$\frac{\partial^2u}{\partial z^2} + 2ik\frac{\partial u}{\partial x} + k^2(n^2-1)u = 0 \quad (7)$$

Where equation (7) is the standard parabolic equation.

Equation (7) by method of separation of variables can be written as

$$2ik\frac{\partial u}{\partial x} = (1-n^2)k^2u - \frac{\partial^2 u}{\partial z^2} (8)$$

Which can be expressed as

$$\frac{\partial u}{\partial x} = i\left\{(1-n^2)k^2 - \frac{p^2}{2k}\right\}u (9)$$

Let consider $A = (1-n^2)k^2 - \frac{p^2}{2k}$ and substitute A into equation (9). This yields

$$\frac{\partial u}{\partial x} = iAu (10)$$

Taking like terms

$$\frac{\partial u}{u} = iA\partial x (11)$$

The solution of the parabolic wave equation becomes

$$u(x_0 + \Delta x, z) = u(x_0)e^{iA\Delta x} (12)$$

It is worthy of note that equation (7) can be factored out to obtain

$$\left\{\frac{\partial}{\partial x} + ik(1-Q)\right\}\left\{\frac{\partial}{\partial x} + ik(1+Q)\right\} (13)$$

This gives us

$$\frac{\partial u}{\partial x} = -ik(1-Q) (14)$$

$$\frac{\partial u}{\partial x} = -ik(1+Q) (15)$$

Where Q is the pseudo-differential operator and is defined by

$$Q = \sqrt{\frac{1}{k^2}\frac{\partial^2}{\partial z^2} + n^2(x,z)} (16)$$

Equation (14) is the outgoing parabolic equation and equation (15) is the incoming parabolic wave equation.

Considering the propagation medium as homogeneous with refractive index n, the field component Ψ satisfies two-dimensional scalar wave equation

$$\frac{\partial^2 \psi}{\partial z^2} + 2ik\frac{\partial^2 \psi}{\partial x^2} + k^2n^2(z,x) = 0 (16)$$

The refractive index varies with the range x and height z and equation (16) is a good approximation provided n varies slowly with wavelength. It is worth noting that equation (16) is not exact [Levy]. If the propagation medium is vacuum, the standard parabolic wave equation in (7)

$$\frac{\partial^2 \psi}{\partial z^2} + 2ik\frac{\partial u}{\partial x} = 0 (17)$$

The solution of equation (1.43) can be expressed as

$$u(x_0 + \Delta x, z) = u(x_0)e^{i\frac{p^2}{2k}\Delta x} (18)$$

V. THE SPLIT STEP FOURIER TRANSFORM SOLUTION

The split-step Fourier method is a very efficient PEM which separate the refractive effect from the diffractive part of the propagator. Considering a two-dimensional scalar wave equation for horizontally and vertically polarised wave. Hardin et.al introduced the split-step Fourier method which transforms the rough surface problem with propagation through a sequence of phase screens [14-17].

The standard parabolic equation (SPE) in equation (7) can be written as

$$\frac{\partial u}{\partial x} = \frac{ik}{2}\left\{\frac{1}{k^2}\frac{\partial^2}{\partial z^2} + (n^2(x,z) - 1)\right\}u (19)$$

Let

$$A = \frac{1}{k^2}\frac{\partial^2}{\partial z^2} (20)$$

$$B = n^2(x,z) - 1 (21)$$

Equation (19) becomes

$$\frac{\partial u}{\partial x} = \frac{ik}{2}\{A+B\}u (22)$$

The analytic solution of the SPE is

$$u(x+\Delta x, z) = u(x,z)e^{\frac{ik}{2}\Delta x(A+B)} (23)$$

Using

$$\delta = \frac{ik\Delta x}{2} (24)$$

Equation (24) yields

$$u(x+\Delta x, z) = u(x,z)e^{\delta(A+B)} (25)$$

Equation (25) is the split-step solution which represent the field propagating through series of phase screens. The field is first propagated through a slice of homogeneous medium characterised by the exponent of A.

The SSFM routine was implemented to propagate the plane wave

$$E(z_0, x, y) = E(z, x, y)exp\left(ik_x + ik_y + ik_z z\right) (26)$$

with E(z, x, y) ≈ 1 along the forward +z direction.

The plane wave was propagated through five (5) 2D slices of sea foam layers each containing isotropically distributed bubbles. The slices are equally dimensioned with area 100mm × 100mm with layer thickness δ_t = 10 mm separating adjacent layers. The foam layer thickness d ≫ λ_0 is required to account for attenuation (E-field amplitude variation) and diffuse scattering (E-field phase variation) as the incident E-field travels through slices of the sea foam layer. WindSat frequency channels (6.8 GHz, 18.7 GHz, 23.8 GHz) were used for propagation of the E-field through slices of sea foam layers.

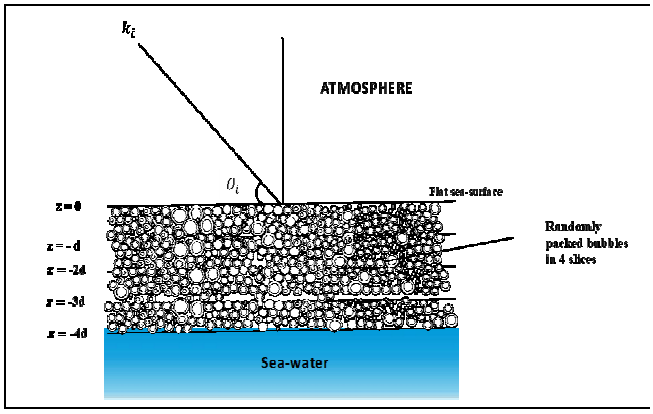

Fig. 1 Geometric configuration of foam-covered sea-surface divided into slices of sea-foam layers.

The incident wave is tilted from the normal so that there is an initial phase gradient along the surface of the sea foam model. This is done by assigning values of $0 \leq \theta_i \leq 90^\circ$ for the zenith angle and fixed azimuthal angle for example $\varphi_i = 0^\circ$ or 45°.

For each of the angles θ_i we compute the E-fields that emerges from the foam layer and calculate the FFTs of the fields. The contour plots of the intensity of the scattered field is displayed. Range of the depths of foam for realistic scenarios were observed to investigate the influence of the foam as a thin phase scattering screen and deep phase scattering screen.

VI. MILLIMETER WAVE ATTENUATION AT LOW AND WINDSAT FREQUENCIES AS A FUNCTION OF DEPTH OF SEA-FORM

The attenuation of the field intensity in decibel (dB) at a low frequency of 6.8 GHz and sea foam slice thickness $\delta_t = 0.1\ mm$ which describes a thin phase scattering screen, as phase perturbation increases as the depth of sea foam layer increases. Fig. 2 and 3 illustrate the variation of attenuation of the E-field in dB with depth in mm of sea-foam layer. This is due to increase in diffuse reflections or scattering as the EM wave interacts with randomly oriented sea-foams with different refractive indices. This happens for both TE and TM polarized E-fields.

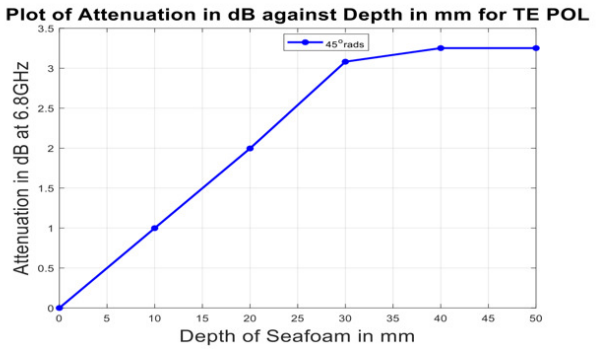

Fig. 2 Attenuation of Field Intensity for horizontal polarization (TE) with zenith $\theta_i = 45°$ and azimuth $\phi = 0°$ with depth of sea-foam at 6.8 GHz and foam layer thickness $\delta_t = 0.1\ mm$.

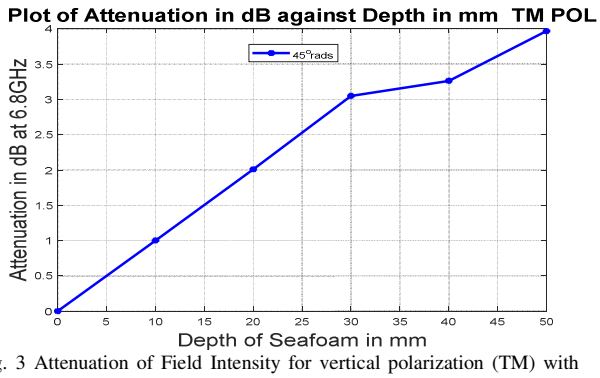

Fig. 3 Attenuation of Field Intensity for vertical polarization (TM) with zenith $\theta_i = 45°$ and azimuth $\phi = 0°$ with depth of sea-foam at 6.8 GHz and foam layer thickness $\delta_t = 0.1\ mm$.

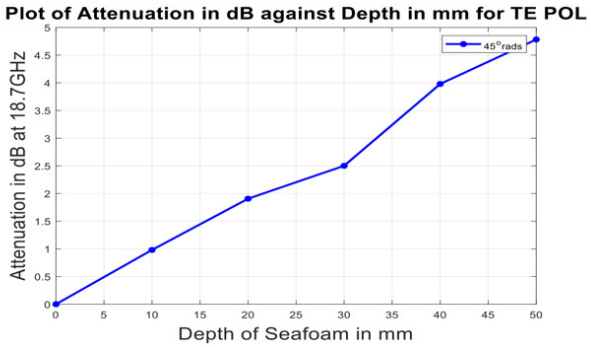

Fig. 4 Attenuation of Field Intensity for horizontal polarization (TE) with zenith $\theta_i = 45°$ and azimuth $\phi = 0°$ with depth of sea-foam at 18.7 GHz and foam layer thickness $\delta_t = 0.1\ mm$.

Similarly, the attenuation of the field intensity in decibel (dB) at WindSat frequency of 18.7 GHz and sea-foam slice thickness $\delta_t = 0.1\ mm$ increases as the depth of sea foam layer increases. Fig. 4 and 5 illustrate the variation of attenuation of the E-field in dB with depth in mm of sea-foam layer. This is also due to increase in diffuse reflections or scattering as the EM wave interacts with randomly oriented sea-foams with different refractive indices. This happens for both TE and TM polarized E-fields.

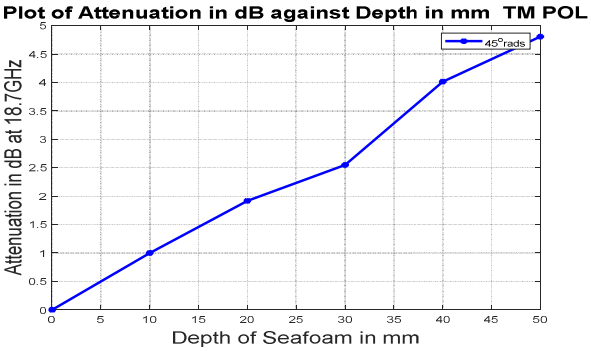

Fig. 5 Attenuation of Field Intensity for vertical polarization (TM) with zenith $\theta_i = 45°$ and azimuth $\phi = 0°$ with depth of sea-foam at 18.7 GHz and foam layer thickness $\delta_t = 0.1\ mm$.

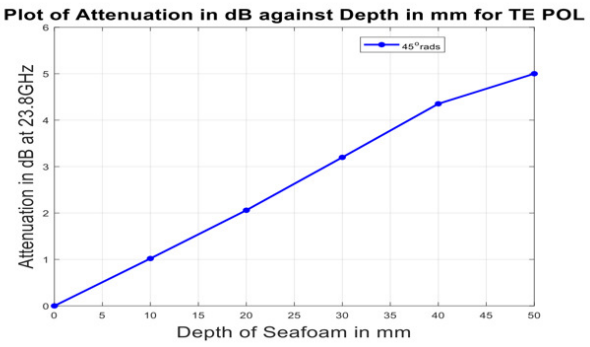

Fig. 6 Attenuation of Field Intensity for horizontal polarization (TE) with zenith $\theta_i = 45°$ and azimuth $\phi = 0°$ with depth of sea-foam at 23.8 GHz and foam layer thickness $\delta_t = 0.1\ mm$.

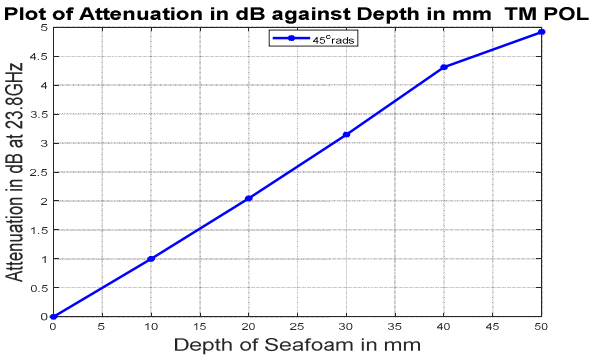

Fig. 7 Attenuation of Field Intensity for vertical polarization (TE) with zenith $\theta_i = 45°$ and azimuth $\phi = 0°$ with depth of sea-foam at 23.8 GHz and foam layer thickness $\delta_t = 0.1\ mm$.

For thin phase scattering screens $\delta_t = 0.1\ mm$ with a given zenith angle $\theta_i = 45°$ and azimuth $\phi = 0°$, the attenuation $\alpha(dB)$ increases with depth (mm) of sea-foam and frequency at 23.8 GHz. The attenuation at 18.7 GHz is less than that at 23.8 GHz, which agrees with the fact that there is more interaction of the E-field with the particles at high frequency. In Fig. 6 and 7, attenuation of the E-fields for both TE and TM polarizations are due to phase perturbations due to diffuse scattering of disordered air-bubbles with varying dielectric constants

VII. CONCLUSIONS

We have shown from our results that attenuation of the E-field is due to diffuse scattering when the incident E-field is multiple reflected by sea-foam as it propagates through the various slices of sea-foam layer. The E-field travels through different paths

and is scattered due to re-radiation of the dipole moments of the disoriented scatterers which absorbs some of the incident E-field and re-radiates it at various directions. The varying effective dielectric constants of the particles enhances diffuse scattering of the incident and transmitted E-fields within the sea-foam layer. The split-step Fourier transform method is a range marching technique that is suitable for evaluation of the E-field propagation given an initial range, the expected depth of the field can be computed as a function of range and depth. Future works will evaluate variation of the field intensity due to its interaction with rough sea-surface covered by foams.

ACKNOWLEDGMENT

Theauthors are gratefulto the reviewers and Executive Editor-in-chief for their insightful comments, which have helped improved the paper. This research work was supported by the Tertiary Education Trust Fund (TETFUND), Nigeria.

REFERENCES

[1] M. D. Anguelova, "Complex Dielectric Constant of Sea Foam at Microwave Frequencies", Journal of Geophysical Research, Vol. 133, C08001, 2008.

[2] M. D. Anguelova, M. Bettenhausen, and P. Gaiser. "Passive remote sensing of sea foam using physically-based models",*2006 IEEE International Symposium on Geoscience and Remote Sensing*, IEEE, 2006.

[3] M. D. Anguelova, "Passive remote sensing of oceanic whitecaps: Further developments", *AGU Fall Meeting Abstracts*. 2013.

[4] A. Stogryn, "The emissivity of sea foam at microwave frequencies ", *Journal of Geophysical Research,* vol. 77, no. 9, 1658–1666, 1972.

[5] Y. Xiaobin, et al. "Optimization of L-band sea surface emissivity models deduced from SMOS data." *IEEE Transactions on Geoscience and Remote Sensing*, vol. 50.5, pp. 1414-1426, 2012.

[6] D. Chen, L. Tsang, L. Zhou, S. C. Reising, W. E. Asher, L. A. Rose, K.-H. Ding, and C.- T. Chen, "*Microwave emission and scattering of foam based on Monte-Carlo simulations of dense media",* Geoscience and Remote sensing, *IEEE Transanction on*, vol. 41, no. 4, 782–790, 2003.

[7] C. Chi-Te, et al. "Analytical and numerical methods for the scattering by dense media. " IGARSS 2000. *IEEE 2000 International Geoscience and Remote Sensing Symposium. Taking the Pulse of the Planet*: *The Role of Remote Sensing in Managing the Environment. Proceedings(Cat. No. 00CH37120*) (vol. 5, pp. 2359-2361). IEEE, 2000.

[8] A. Benjamin and D. O. Bebbington, "Millimeter wave propagation and attenuation in closed packed sea foam layer and complex dielectric constant of sea-foam using split-step Fourier transform", *Progress in Electromagnetic Symposium-Fall (PIERS-FALL), IEEE*, 2556-2553, 2017.

[9] G. Apaydin and L. Sevgi. "The Split-step Fourier and finite element based parabolic equation propagation prediction tools: Canonical tests, systematic comparisons, and calibration," *IEEE Antennas and Propagation Magazine*, vol. 52, No. 3, 66-79, 2010.

[10] M. Levy. " Parabolic equation method for electromagnetic propagation," IEEE Electromagnetic Wave Series, vol. 45, *The Institute of Engineering and Technology*, Dec. 2000.

[11] G.F.,Williams,"Microwave emissivity measurements of bubbles and foam., IEEE Trans. Geosci.., Remote Sensing, Electron"., vol.9, 221-244, 1971.

[12] P.C. Pandey and R. K. Kakar. "An empirical microwave emissivity model for a foam-covered sea",Remote sensing of the ocean,vol.**7**, no.3,135-140, IEEE J Oceanic Eng, 1982.

[13] X. Z. Huang and Y. Q. Jin, "Scattering and emission from two-scale randomly rough sea surface with foam scatterers",Proc. Inst. Elect. Eng., Microwave Antenna Propagat., vol.142,109-114, 1995.

[14] S. L. Durden and J. F. Versecky, "A physical radar cross-section model for a wind driven sea with swell", *Ocean Engineering, IEEE Journal of, vol.*10, no.4,445-451, 1985.

[15] K. H. Ding, L. Tsang and Q. Li, "Computational electromagnetic scattering models for microwave remote sensing", *Encyclopedia of RF and Microwave Engineering*, 2005.

[16] Wilheit Jr.,"A model for the microwave emissivity of the ocean's surface as a function of wind speed",Geosci. Electron. IEEE Trans. vol.17**,** 244-249, 1979.

[17] J. Guo, L. Tsang, W. Asher, K.-H. Ding, and C.-T. Chen, "Applications of dense media radiative transfer theory for passive microwave remote sensing of foam-covered ocean," Geoscience and Remote Sensing,IEEE Transactions on, vol.39, no. 5, 1019–1027, 2001.

